Comparison of the thermal performances of two nanofluids at low temperature in a plate heat exchanger

Thierry Maré, Halelfadl Salma, Sow Ousmane, Patrice Estellé, Steven Duret, Bazantay Frederic

HAL Id: hal-00667139

https://hal.science/hal-00667139

Submitted on 18 Jul 2012

Comparison of the thermal performances of two nanofluids at low temperature in a plate heat exchanger

Thierry Maré [*a] Salma Halelfadl [a] Ousmane Sow [b], Patrice Estellé [c],

Steven Duret [d], Frederic Bazantay [d]

[a]UEB, LGCGM, Equipe Matériaux et Thermo-Rhéologie, INSA/Université Rennes 1, IUT de Saint-Malo, Rue de la Croix Désilles, CS51713, 35417 Saint-Malo Cedex, France

[b]Laboratoire Matériaux Mécanique et Energétique (LMME), Ecole Polytechnique de Thiès (EPT), Thiès, Sénégal

[c]UEB, LGCGM, Equipe Matériaux et Thermo-Rhéologie, INSA/Université Rennes 1, IUT de Rennes, 3 rue du Clos Courtel, BP 90422, 35704 Rennes Cedex 7, France

[d]Pôle Cristal, Centre Technique Froid et Climatisation, 22100 Dinan, France

[*] Corresponding Author

Abstract

The objective of this study is to compare experimentally the thermal performances of two types of commercial nanofluids. The first is composed of oxides of alumina ((γAl_2O_3)) dispersed in water and the second one is aqueous suspensions of nanotubes of carbons (CNTs). The viscosity of the nanofluids is measured as a function of the temperature between 2 and 10°C. An experimental device, containing three thermal buckles controlled in temperature and greatly instrumented permits to study the thermal convective transfers. The evolution of the convective coefficient permits to study the convective thermal transfers. The evolution of the convective coefficient is presented according to the Reynolds number, at low temperature from 0 to 10°C and for the two aforementioned nanofluids. An assessment of the pressure drops in the circuit as well as of the powers of the circulator and outputs is dealt with.

Keywords:

Nanofluid**,** nano particles, viscosity, transfers of convective heat, exchanger of heat plates, pressure drop, experimental.

1. Introduction

The efforts aiming at improving the thermal exchangers in many industrial sectors (automobile, building, electronic...) require the intensification of the heat transfers, Padet [1]. The "passive" improvements at the level of the exchange surfaces have already been extensively explored and have reached their objective limits. In the case of the coolant fluids, the thermal conductivity is one of the first parameters to take in account to value the potential of heat exchange. However the more used fluids such as water, the ethylene-glycol and oil possess a relatively weak thermal conductivity. New ways of optimization consist in using new fluids named "Nanofluids" capable of improving the thermal transfers. The nanofluids are colloïdal solutions composed of metallic particles of nanometric size in suspension in a base liquid. Choi [2] was probably the first to qualify these nanofluids.

To explain the improvement of thermal conductivity that the presence of the nano particles brings in these fluids, Keblinski [3] and Eastman [4], lean on the study of the Brownian movement and the effects at the solid/liquid interfaces. Xuan [5] explains this improvement

2

of conductivity by the collision of the particles. The experimental studies done so far, are essentially about the measure of the thermal conductivity [6] [7], and the measure of the viscosity [8] [9]. Some articles study numerically and experimentally the thermal transfers in tubular exchangers [10] [11].

To limit the phenomena of agglomeration, the manufacturers add to these fluids a non-negligible part of surfactant. The viscosity is impacted by this surfactant, and the literature shows that it is difficult to control the spread of the particles and that the usual relations expressing the viscosity don't apply for elevated volumic concentrations. Khaled [12] studies the importance of the dispersion and its experimental results show an influence of the surfactant of more than 20% on the number of Nusselt obtained.

When looking at the experimental results, we notice that the usual theoretical relations for the fluids with particles don't apply to the case of the nanofluids, and the experimental study on the thermo physical properties shows important disparities according to the methodology of measure and mixture, sometimes even for the nanofluids. [13] [14] [15].

With regard to the thermal transfers by convection, some studies show an improvement in presence of nanoparticules [15] [16], whereas other studies observe a reduction of these transfers [17]. Ding and al. [18] measured the convective heat transfer coefficient of aqueous suspensions of CNTs in a horizontal tube and reported that for the nanofluids containing 0.5%wt CNTs, its enhancement rate to water was over 350%. Several reviews of nanofluids show that the associated thermal transfers are not very much understood [19]. Vijjha and al. [20] showed in a numerical work simulating the heat performance in a flat tubes of a radiator. For this exchanger heat transfer rate increase up to around 94% by adding 10% Al_2O_3 nanofluid and increase up to around 89% by adding 6% CuO nanofluid.

It can be noted that the few existing experimental and numerical studies on the thermal transfers by convection are mainly concerned with convective transfers in the tubes and that the case of the plate heat exchangers is little, or not, taken in account. We can also note that the range of temperature used in the experimental studies is comprised between 20°C and 60°C.

There are only few works which correlate a competition between thermal performance (heat transfer) and pressure drop to clarify the practical contribution of nanofluid [20]. In addition to this, the thermal behavior of these fluids in forced convection around a plate at low

3

temperatures (lower to 20°C) doesn't seem to have been studied. The objective of the present work is to study and compare the practical benefits, as a competition between heat transfer enhancement and pumping power losses, caused by the use of two nanofluids in a plate heat exchanger at low temperatures. The two types of commercial nanofluids used are composed of alumina (γAl2O3) dispersed in water and aqueous suspensions of nanotubes of carbons (CNTs). The determination of the viscosities is obtained experimentally for temperatures lower than 10°C. An experimental device, containing three thermal buckles controlled in temperature and greatly instrumented, and two plate heat exchanger, permits to study the convective thermal transfers. The evolution of the convective coefficient is presented according to the number of Reynolds for a range of active temperature between 0°C and 10°C and for the three aforementioned nanofluids. An assessment of the pressure drops in the circuit as well as of the powers of the circulator and outputs is dealt with.

2. Experimental set up

2.1. Experimental system

The experimental installation, presented on the figure 1 and schematized on figure 2, is constituted of three buckles (hot buckle, central buckle, cold buckle) and two identic plate heat exchangers (1), (2). The central buckle is equipped with an UPS circulator 60 Grundfos with three speeds (6) assuring a flow rate between 400 to 1000 l/h, of an ultrasonic flow meter (8) and of four PT100 probes permitting the measure of 4 temperatures (Tce, Tcs, Tfe, Tfs). Distilled water in the case of the validation of the installation as well as the different nanofluids will circulate in this buckle. The ultrasonic flow meter (extrusive) is calibrated on the distilled water and our knowledge on the thermo physical properties of nanofluids doesn't permit to adapt it to the flow of our fluids. On the other hand, this flow meter will serve for the validation of the installation on water. The flow of the nanofluids will be determined by calculation of the thermal balances and the equation (6).

The production of heat is assured by a *vulcatherm vulcanix* of a calorific power of 2KW with a range of temperature comprised between 10 and 90°C, in the hot buckle (V indication). Two PT100 probes permit the measures of the entry and exit temperatures of the exchanger (Tve, Tvs). The coolant fluid is water and a system of regulation permits to control the entry temperature Tve intersection (hot side). The volumic flow rate (Qv1) is measured by an electromagnetic flow meter**.**

The thermal balances are made in the exchanger 1 between the central buckle and the hot buckle. In order to control the entry temperature of the exchanger (1) cold side (Tce), we have a cold buckle (subscript T) and a regulation system. The cold buckle of a circulator is constituted of a refrigerated group (Trane) of 25 KW power, a buffer tank, a regulator with brass valve (not visible on the diagram) and a floodgate three ways Siemens VXG 44 (9) equipped with an SQS65 Siemens servomotor and of a SYNCO 100 Siemens regulator. The three- way valve controls the glycol water output in this buckle according to the temperature of Tfs order (left exchanger 2 central buckle sides). The system being thermally isolated the Tfs temperature is close to the entry temperature of exchanger 1, Tce. The temperatures are measured by two PT100 (Tte, Tts) probes.

So as not to disrupt the measures of temperatures by the side effects in the circuit, all PT100 probes are placed in exit elbow in accordance with the recommendations of the NF EN 306 norm. The probes and the flow meter are joined to a power station of acquisition acted 34970A permitting a temperature precision of 0.1°C, of 0.5% on the electromagnetic flow meter and 0.1% on the ultrasonic flow meter (calibrated on water) on the whole acquisition chain, acquisition frequency being measured every 5 seconds.

The two plate heat exchangers used in this experimentation are identical and of SWEP E5T type [21]. They are composed of 20 plates 0.3 mm thick, 7.1 mm wide, the space between every-plate measures 1.94 mm and the total surface of exchange measures 0.216 m2 (figure 3). The constituent material of the exchange is the AS130 and its conductivity is of 16.3 W/ mK.

2.2. Validation of the installation

To evaluate the thermal losses or gains generated by the thermal isolation of the experimental installation, a validation is done while making water flow in the central buckle. Several data acquisitions are done while maintaining the hot temperature Tve at 15°C and the cold temperature Tfs at 3°C. The acquisition is made at a pace of 5 seconds during 2300 seconds. The stability is obtained after 1000 seconds. Figure 4 presents the evolution of the temperatures of the installation according to the time for a water flow in the central buckle of 0.28 l/s and in the hot buckle of 0.205 l/s. The flow in the cold buckle (T) varies according to the opening of the automatic three-way valve in order to get a constant temperature Tfs.

We notice a stability of 0.1°C on set point input of the exchanger at the hot side Tve. A precision of 0.5 °C is obtained on the exit temperature of the exchanger 2 at the central buckle side. One can note for the evolution of temperatures in the central buckle a gap by pairs of temperatures Tfe, Tcs and Tce, Tfs of 0.1 °C equal to the measure we reach with precision. It shows that the pipelines of the installation are well thermally isolated and it validates the fact that the regulation on the Tfs temperature is acceptable.

At the level of the heat insulation of the exchanger (1), a validation is done while making water circulates in the central buckle and in the hot buckle. The assessment of the thermal gains, noted Φ_+, brought by the external environment in our exchanger is determined by the equation of balance of the heat power.

$$\phi_+ = \phi_v - \phi_c = Q_{m_v} C_{pv} (T_{vs} - T_{ve}) - Q_{m_c} C_{pc} (T_{ce} - T_{cs}) \tag{1}$$

Several tests have been done for several flows (400, 600, 800 and 1000 l/h) in the central buckle and a flow in the hot buckle (0.205 l/s), the temperatures are imposed to 3°C for Tfs and 15°C Tve. The results, figure 5, are presented in a dimensionless shape while drawing the evolution of the relation between the gain of heat flux brought by the external environment and the flux of initial heat at the hot side ϕ_+ / ϕ_v, according to the logarithmic gap in exchanger (1). The logarithmic gap of the temperatures ΔT_{LM} is given by the following relation:

$$\Delta T_{LM} = \frac{(T_{vs} - T_{ce}) - (T_{ve} - T_{cs})}{\ln\left(\dfrac{T_{vs} - T_{ce}}{T_{ve} - T_{cs}}\right)} \tag{2}$$

We notice that in the low temperatures scales considered in our experimentations, the gain in power presents 3.5% (average value) of the power exchanged in the hot side. This value will be taken in account in the energizing balances in presence of nanofluids and it confirms that our installation is relatively well heat insulated.

3. Calculation and procedure for measuring

3.1. Nanofluids properties

The nanofluids studied in this present work are constituted of demineralized water, of nanoparticules of alumina (γAl_2O_3) or nanotubes of carbon and of a third component named

surfactant. In this work we suppose that the surfactant has a little influence on the density and the heat capacity of the nanofluids and that the viscosity is impacted by this surfactant.

The nanofluids N1 and N2 used, have as basic fluids water PH5 and the characteristics of their nano particles are presented in table1.

In this present work, the thermal conductivity is not involved in our calculations, so we do not need to measure or determine it.

- **The density**

We consider the density of the particles as constant in the range of temperature used, and we take in account the variation of the density of the water in accordance with the temperature. We neglect the presence of surfactant and the relation used is the following:

$$\rho_{nf} = (1 - \varphi_v)\rho_{bf} + \varphi_v\rho_p \tag{3}$$

- **The heat capacity**

The specific heat of the nanofluids was obtained from the equation given by Xuan and al. [22] which assumes thermal equilibrium between the base fluid and the nanoparticules. The equation is:

$$(C_p)_{nf} = (1 - \varphi_v)(C_p)_{bf} + \varphi_v(C_p)_p \tag{4}$$

- **Dynamic viscosity**

It seems that the differences of the experimental data on the measure of viscosity of the nanofluids observed in the literature are not adequate with the usual two-phase relations [23]. Therefore, the viscosity will be measured experimentally.

The rheological study was made for two reasons: to measure the dynamic viscosity and to control the stability of suspensions. All Rheological measurements were performed using a Malvern Kinexus Pro Rheometer equipped with parallel plate geometry under controlled temperature. The diameter of the plates is 40 mm and the gap is 0.5mm. The temperature was controlled using a peltier temperature control device located below the lower plate with an accuracy of 0.01°C. Stress-controlled measurements were performed imposing a logarithmic

7

stress ramp increase followed by a reverse stress decrease. The stress was increased, before the reverse stress decrease, from 10^{-3} to 15 Pa and 30 Pa, respectively for N1 and N2. Preliminary studies have validated the applicability of the maximum shear stress (15 and 30 Pa) depending on the nanofluid used, in order to avoid sample ejection and maintain a constant normal force during experiments. To assess the effect of the surfactant and the stability of the nanofluids, several measurements were carried out on several samples of each nanofluid under the same shear stress range.

- **Dispersion of nanoparticules**

To control the dispersion of nanoparticles in our commercial nanofluids, a study based on measuring the size of the nanoparticles by dynamic light scattering was performed. This method can detect the presence of agglomerates [24]. Dynamic Light Scattering (DLS) measurement was here performed on the nanofluid by using a Zetasizer Nano S (Malvern Instruments). Figure 6 shows the evolution of the nanoparticles size with the intensity distribution. The measured average particle size in the nanofluids is much larger than that of the primary nanoparticles, as described in table 1. The average cluster size for the Al_2O_3 water based nanofluid is 400 nm. The average agglomerate sizes for the CNT water based nanofluid is centered around 400 nm. The first peak could be attributed to particles in random position. These results show that our commercial nanofluids and nanoparticles are not well dispersed.

3.2.   Calculation of convective heat transfer

The tests consisted in measuring the different temperatures at the level of every buckle, as well as the flow rate in the hot circuit. These measures have been done for the same external conditions as for the preceding Water-water validation test (same temperatures of order hot side and cold side), and for several flow rates in the central buckle.

The nanofluid mass flow rate Q_{m_c} at the central buckle is deduced of the received thermal power ϕ_c. The calorific power received by the nanofluid at the level of the exchanger 1 is equal to the power lost by water at the hot buckle to which we add the external power received ϕ_+ according to the temperatures logarithmic gap (figure 5).

$$\phi_c = Q_{m_v} C_{pv} \left(T_{vs} - T_{ve} \right) + \phi_+$$

(5)

The mass flow rate of the nanofluid is obtained in the following manner:

$$Q_{m_c} = \frac{\phi_c}{C_{pc}\left(T_{fs} - T_{fe}\right)} \qquad (6)$$

- . Calculation of the convective heat coefficient

To determine the h convection coefficient in the cold buckle, we use the following method:

$$h_{nf} = \frac{1}{\left(\dfrac{S_x \Delta T_{LM}}{\phi_c} - \dfrac{1}{h_w} - \dfrac{e}{k}\right)} \qquad (7)$$

The h_w water coefficient in the hot buckle is determined by:

$$h_w = \frac{Nu k_w}{D_h} \qquad (8)$$

With

$$D_h = \frac{4S}{p} \qquad (9)$$

S and p are respectively the section of passage between the two plates and the wet perimeter.

$$Nu = B \, \mathrm{Re}^r \, \mathrm{Pr}^{\frac{1}{3}} \qquad (10)$$

While taking a corrugation angle of 60° at the level of the plates and respectively for B and r, the values 0.455 and 0.66, these values are issued from the standardization on the water of the exchanger by the constructor.

The numbers of Reynolds and Prandlt are respectively:

$$\mathrm{Re} = \frac{\rho_w V D_h}{\mu_w} \; ; \mathrm{Pr} = \frac{\mu_w C_{pw}}{k_w} \qquad (11)$$

The velocity in the hot circuit (of water) is obtained by:

$$V = \frac{Q_{m_v}}{n \rho_w S} \qquad n=10 \qquad (12)$$

9

The velocity of the nanofluid is calculated in the following manner:

$$V = \frac{Q_{m_c}}{n \rho_{nf} S} \qquad n=9 \tag{13}$$

With n is the number of channels (9 or 10, according to hot or cold fluid, in our case, water is from the hot side of the exchanger).

- **Experimental uncertainly measure of h**

The absolute uncertainties on the PT 100 probes and relative on the electromagnetic flow meter are respectively of $\Delta T = 0.1$ °C: $\dfrac{\Delta Q_{V1}}{Q_{V1}} = \pm 0.5\%$ and this on the whole acquisition chain. While neglecting the water thermo physical uncertainties coefficients the relative uncertainty the convective transfer coefficient in the hot side is estimated to 1% by the constructor of the exchanger. While considering the relation (8) and the mistakes in temperature stabilities given by the figure 4, we get a relative uncertainty on the convective transfer coefficient h_{nf} in the nanofluid of 10%.

3.3. Calculation of pressure drops

To characterize the pressure drops of the plate heat exchanger we use the relation (14) that expresses the total loss of load in meter of fluid column comprising the losses of linear and singular pressure drops:

$$\Delta H = \lambda \frac{L}{D_h} \frac{V^2}{2g} + K \frac{V^2}{2g} \tag{14}$$

In order to facilitate the calculations, we introduce the equivalent length to define the coefficient of singular load loss, equation (15).

$$L_{eq} = K \frac{D_h}{\lambda} \tag{15}$$

The total load loss in our exchanger is therefore:

$$\Delta H = \lambda \frac{\left(L + L_{eq} \right) V^2}{D_h \quad 2g} \tag{16}$$

The merely theoretical assessment of the losses of singular loads is difficult because of the complexity of the studied system (pipes, corrugations). We define an A constant regrouping the complex geometric features of the exchanger (figure 3) and taking into account the singular pressure drops.

$$A = \frac{\left(L_{eq} + L\right)}{2gD_h}$$

(17)

The equation (15) becomes

$$\Delta H = A\lambda V^2$$

(18)

To determine λ we apply the Poiseuille relation for a laminar flow

$$\lambda = \frac{64}{\text{Re}}$$

(19)

To determine A, we determine the total pressure drops ΔH with the help of the constructor's software for three validated fluids and having viscosities of the same order of size as our nanofluids (water / ethylene glycol 40%, milk, water/ sugar 30%). When doing the report between ΔH and λV^2, we get in every case a value of the coefficient A of 2169.5 S^2/m with a precision of 5%.

These pressure drops generate a power of the circulator determined by the following relation:

$$P_u = g\Delta H Q_{m_c}$$

(20)

To study the practical benefits of using the nanofluids quantitatively, we introduced the parameter ξ which evaluates the gain, in comparison with water, in term of a competition between heat transfer enhancement and pumping power loss.

$$\xi = \frac{\left|\left(\phi_c - P_u\right)_w - \left(\phi_c - P_u\right)_{nf}\right|}{\left(\phi_c - P_u\right)_w}$$

(21)

11

4. Results and discussion

4.1. Viscosity of nanofluids

The measurements were performed at four temperatures, 2°C, 5°C, 7°C and 10°C, and varying also the time of shear stress ramp: 120s (2 minute), 180s (3 minute), 240s (4 minute) and 300s (6 minute). This is made for both investigating the influence of low temperature and shearing time on the rheological properties of the nanofluids. The measurements were also duplicated to verify the repeatability of the tests.

Figure 7 presents two evolutions of the shearing velocity according to the constraint of shearing for the N2 nanofluid (nanotube of carbon) at 5°C and for a logarithmic ramp of decreasing constraints. We notice that the values obtained for different samples are very close, which validates our trial protocol and shows that the nanofluid is stable. Besides, the results shown in figure 8 show that CNT nanofluid is Newtonian for high shear rate. Similar tests were performed on the alumina nanofluid N1 and show that for several samples we obtain the same viscosity values. This leads to the conclusion of the nanofluid is stable. Besides, the behavior of these nanofluids is thinning at low shear rate and Newtonian at high shear rates. High shear stress is observed in the plat heat exchanger used in this work due to its geometry. We can therefore deduce dynamic viscosity by the following relation:

$$\tau = \mu \dot{\gamma} \tag{21}$$

Figure 9 shows the relative viscosities obtained for our two nanofluids compared to dynamic viscosity of water and for 4 different temperatures (2, 5, 7 and 10°C).

It can be noticed that the dynamic viscosity decreases when the temperature increases. The viscosity is 3 times superior to the water for N1 and 7 times superior for N2. For our nanofluids, figure 9 shows that the Einstein Model (Eq. 22) fails completely.

$$\mu_{nf} = \left(1 + 2.5\varphi_v\right)\mu_{bf} \tag{22}$$

4.2. Convective heat transfer coefficient of the nanofluids

The tests have been achieved for four Q_c flow rates of nanofluids. The flow rate in the hot side Q_V and its order temperature T_{ce}, are respectively: 750l/h and 15°C. The order temperature in the cold side T_{fs} is fixed at 3°C, the flow rate is adjusted by the regulation on

the three - way valve. The data are checked every 5 seconds on a measuring period of 200 seconds. The average results cover this period and figure 10 shows the evolution of the relative convective transfer coefficient h_{nf}/h_w according to the Reynolds number.

The measures of heat transfer are done in laminar mode (lower Reynolds number). The fluids being very viscous, the Reynolds number obtained are low. When we compare the evolution of the convective coefficients with those of water at the same conditions, we notice an enhancement rate of 42% and 50% for N1 and N2 respectively (table 2).

The viscosity of the nanofluids is quiet higher than the viscosity of water (figure 9), so before the use of these fluids in the thermal exchangers, it is necessary to study the impact of the viscosity on the losses of loads generated. It is therefore important, in the setting of an industrial application, to find the compromise between the gain in thermal transfer and the energetic losses by the setting in motion of the fluid carrier by means of a pump.

4.3.   Pressure drop _ Thermal hydraulic performance

Figure 11 shows the evolution of the pressure drop of the circulator, according to the Reynolds number for N1 and N2 in the central buckle. We notice that for the same Reynolds number the pressure drop can be 7 times superior to that of water for the nanofluid N2 due to its high viscosity and 3 times superior to that of water for the nanofluid N1.

Figure 12 shows the evolution of the practical benefits ξ of N1 and N2 according to the Reynolds number. It can be observed from this figure that the gain can reach 22% for N1 and 150% for N2. This result is very important, it reports that alumina and Carbone nanotubes show a better thermal-hydraulic performance in terms of a competition between heat transfer enhancement and pumping power loss in comparison with pure water.

5. Conclusion

Two nanofluids alumina (γAl$_2$O$_3$) and carbon nanotubes (CNTs) dispersed in water are tested in the experimental process presented previously under a laminar out-flow mode. The experimental installation has been finalized and validated on water in order to value the thermal performances of the nanofluids at low temperature.

The results show an improvement in laminar mode of the convective heat transfer coefficient of about 42% and 50% for N1 and N2 respectively compared to that of pure water for the same Reynolds number. The results show that the impact of the viscosity and the

pressure drop at low temperatures is important and has to take into account before to use nanofluids in heat exchanger. Finally, we observed that the gain can reach 22% for N1 and 150% for N2. This result reports that alumina and Carbone nanotubes show a better thermal-hydraulic performance in terms of a competition between heat transfer enhancement and pumping power loss in comparison with pure water.

Complementary experimental studies on the thermal conductivity would permit to study the evolution of the number of Nusselt according to the number of Reynolds and finally the impact of the surfactant on the thermal characteristics of the nanofluids must be better dominated to analyze in a more precise way the thermal transfers. It's possible that in this low temperature, the surfactant loss these properties.

Nomenclature

C_p: thermal capacity of fluid, J/kg.K.

D_h: hydraulic Diameter, m

Q: volumic flow rate, m^3/s

k : Thermal conductivity of fluid, W/mK

S: flow area, m²

T : Temperature, °C, K

L : lenght, m

Re: Reynolds number, $Re=\rho UD/\mu$

Nu: Nusselt number, hD/k

Pr: Prandlt number, $Pr=C_p\mu/k$

V: fluid velocity, $m.s^{-1}$

K: head losses coefficient

P_u: pumping power loss, W

h : convective coefficient of exchanger,

W/m²K

S_x: exchange area, m²

g: gravity acceleration, m²/s

e: plate thickness, m

L_{eq}: equivalent length, m

ϕ : Thermal power, W

ν : kinematic viscosity of fluid, m²/s

ρ: fluid density, kg/m^3

μ: fluid dynamic viscosity, Pa.s

φ: concentration, %

τ: shear stress, Pa

$\dot{\gamma}$: shear rate, s^{-1}

λ: Linear pressure drop coefficient

ΔH: Pressure drop, m ξ: Practical benefits parameter, %

Subscripts / Superscripts

c: Central   T: Trane   v : volumic   + : gain

e : entry   s : exit   m : mass   LM : logarithmic

V : Vulcatherm   w : water   p : particule   bf : base fluid

nf : Nanofluid

References

[1] Padet J., Echangeur de chaleur, Masson (1994).

[2] Choi, S., Enhancing thermal conductivity of fluids with nanoparticules, In Developments Applications of Non -Newtonians Flows, D.A. Siginer and H. P. Wang. New-York : Americain society of Mechanical Engineers, Vol. 66 (1995), 99-105.

[3] Keblinski P., Phillpot S.R., Choi S.U.S. and Eastman J.A., Mechanisms of heat flow in suspensions of nano-sized particles (nanofluids), Int. J. Heat Mass Transfer 45 (2002), 855–863.

[4] Eastman J.A., Choi S.U.-S., Li S., Yu W. and Thompson L.J., Anomalously increase effective thermal conductivities of ethylene glycol-based nanofluids containing copper nanoparticles, Appl. Phys. Lett. 78 (No 6) (2001), 718–720.

[5] Xuan Y. and Li Q., Heat transfer enhancement of nanofluids, Int. J. Heat Fluid Flow 21 (2000), 58–64.

[6] Murshed S.M.S., Leong K.C. and Yang C., Enhanced thermal conductivity of TiO_2–water based nanofluids, Int. J. Thermal Sci. 44 (2005), 367–373.

[7] Roy G., Nguyen C.T., Doucet D., Suiro S., Maré T., Temperature-dependent thermal conductivity evaluation of alumina based nanofluids, in: Proc. 13th IHTC, 13–18 August 2006, Sydney, Australia.

[8] Nguyen C.T., Desgranges F., Roy G., Galanis N., Maré T., Butcher S. and Angue Mintsa H. Temperature and particle-size depends viscosity dated heart water-based nanofluids - Hysteresis phenomenon, International Journal of Heat of and Fluid Flow 28 (2007), 1492-1506.

15

[9] Marziehsadat H., Ghader S., A model for temperature and particle volume fration effect on nanofluid viscosity, Journal of Molecular Liquids 153 (2010), 139-145.

[10] Ben Mansour R., Galanis N., Nguyen C.T., Experimental study of mixed convection with water–Al_2O_3 nanofluid in inclined tube with uniform wall heat flux, International Journal of Thermal Sciences, 50 (2011), 403-410.

[11] Ben Mansour R., Galanis N. and Nguyen C.T., Effect of uncertainties in physical properties on forced heat transfer with nanofluids, Appl. Therm. Eng. 27 (1) (2007), 240–249.

[12] Khaled A.R.A. and Vafai K., Heat transfer enhancement through control of thermal dispersion effects, Int. J. Heat Mass Transfer 48 (2005), 2172-2185.

[13] Maré T., Schmitt A.-G., Nguyen C.T., Miriel J., Roy G., Experimental heat transfer and viscosity study of nanofluids: water–γAl_2O_3., In: Proceedings of the 2nd International Conference on Thermal Engineering Theory and Applications, Paper No. 93, January 3–6, 2006, Al Ain, United Arab Emirates.

[14] Nguyen C.T., Desgranges F., Galanis N., Roy G., Maré T., Boucher S., Angue Mintsa H., Viscosity data for Al_2O_3–water nanofluid—hysteresis: is heat transfer enhancement using nanofluids reliable? International Journal of Thermal Sciences, 47(2) (2008), 103-111.

[15] Luciu R., Maré T., Sow O., Enhancement of Heat transfer in solar using nanofluid: experimental dated, ICTEA Proceedings of the Fourth International Conference on Thermal Engineering: Theory and Applications, January 12-14, Abu Dhabi, UAE, 2009.

[16] Maïga S.E.B., Palm S.J., Nguyen C.T., Roy G. and Galanis N., Heat transfer enhancement by using nanofluids in forced convection flows, Int. J. Heat Fluid Flow 26 (2005), 530–546.

[17] Zeinali Heris S., Estfahany M.N., Etamad S.G., Experimental investigation of convective heat transfer Al2O3/water nanofluid in circular tube, International Journal of Heat and Mass transfer, 28 (2007), 203-210.

[18]: Ding Y., Alias H., Wen D., Williams R. A., Heat transfer of aqueous suspensions of carbon nanotubes (CNT nanofluids), International Journal of heat and Mass Transfer, 49 (2006), 240-250.

[19] Daungthongsuk W. and Wongwises S., A critical review of convective heat transfer of nanofluids, Renew. Sust. Energ. Rev. 11 (5) (2007), 797–817.

[20] Vajjha R.S., Das D. K., Numburu P. K., Numerical study of fluid dynamic and heat transfer performance of Al_2O_3 and CuO nanofluids in the flat tubes of a radiator, International journal of Heat and Fluid Flow, 31 (2010), 613-621.

[21] http://www.swep.net/

[22] Xuan Y., Roetzel W., Conceptions for heat transfer correlation of nanofluids, International Journal of heat and Mass transfer, 43(2000), 3701-3707.

[23] Pak B., Cho Y. I., Hydrodynamic and heat transfer study of dispersed fluids with submicron metallic oxide particle, Exp. Heat Transfer, 11(1998), 151-170.

[24] Phuoc T.X, Massoudi M., Chen R.H., Viscosity and thermal conductivity of nanofluids containing multi-walled carbon nanotubes stabilized by chitosan. Int. J. of Thermal Science, 50(2011), 12-18.

List of figures:

List of Tables :

Figure 1

[1] : Heat exchanger, hot side   [6] : UPS circulator with three speeds
[2] : Heat exchanger, cold side   [7] : Electromagnetic flow meter
[3] : Central buckle   [8] : Ultrasonic flow meter
[4] : Vulcatherm buckle   [9] : Three-way valves
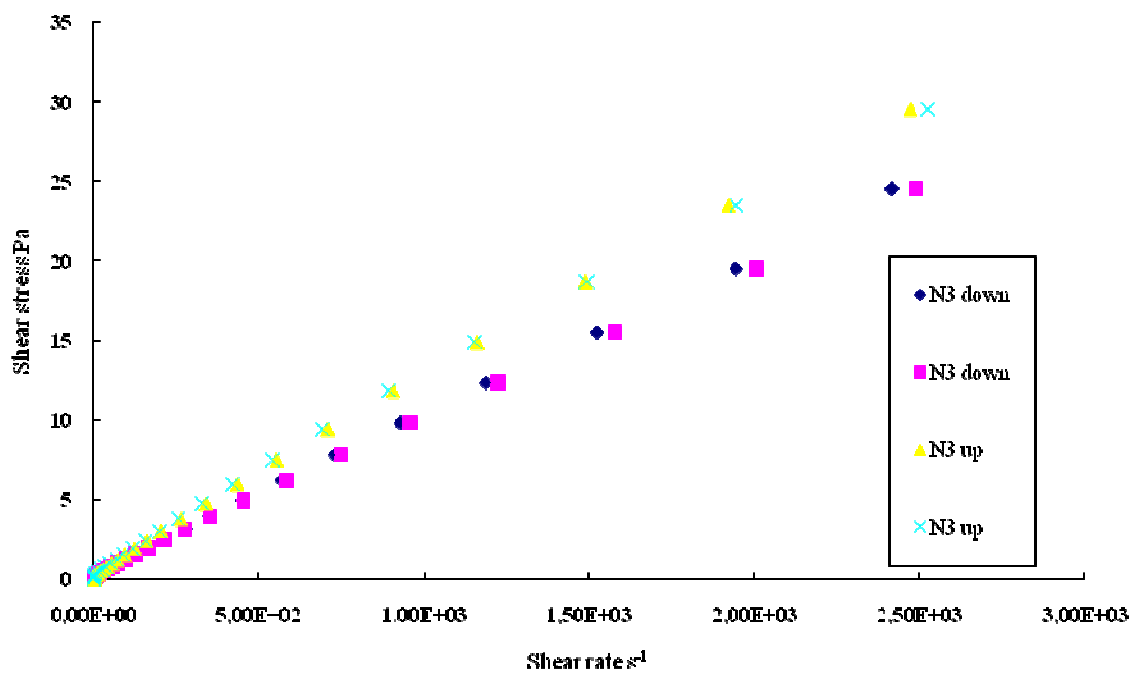[5] : Trane buckle
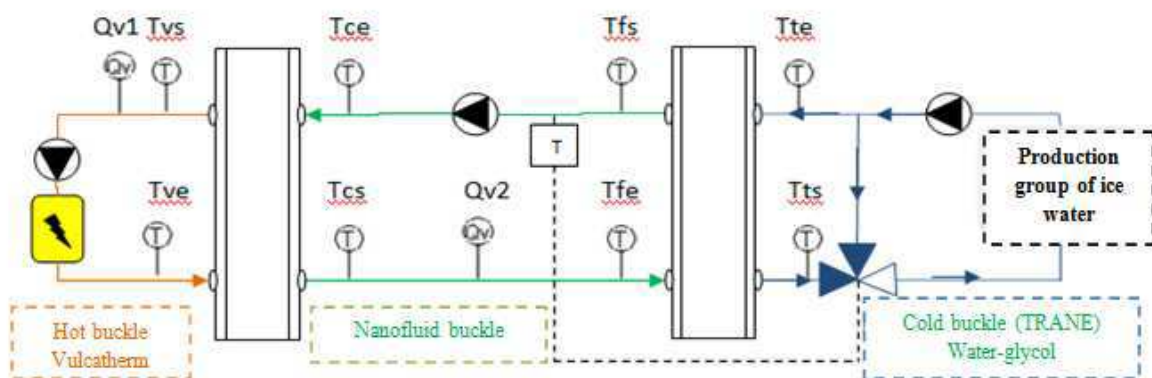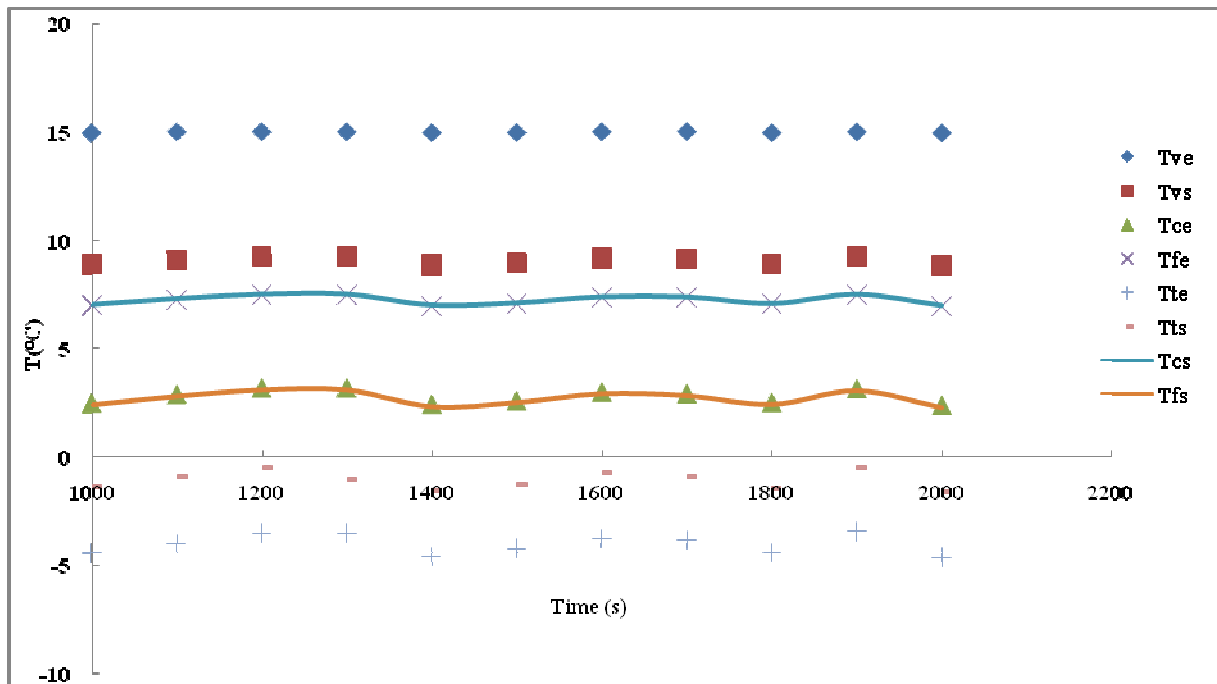
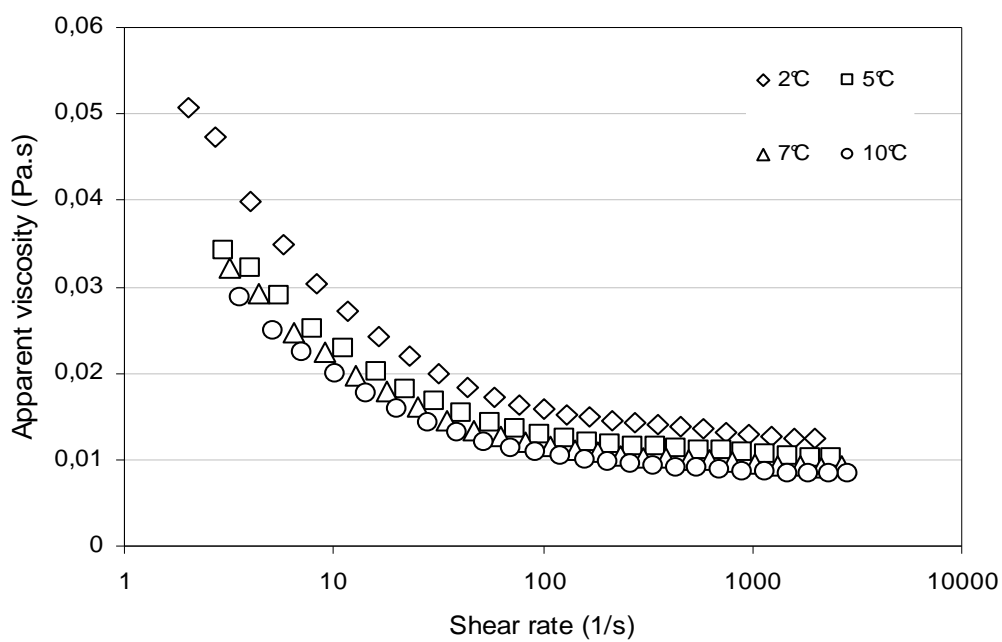*Figure 2 :*

Figure 3 :

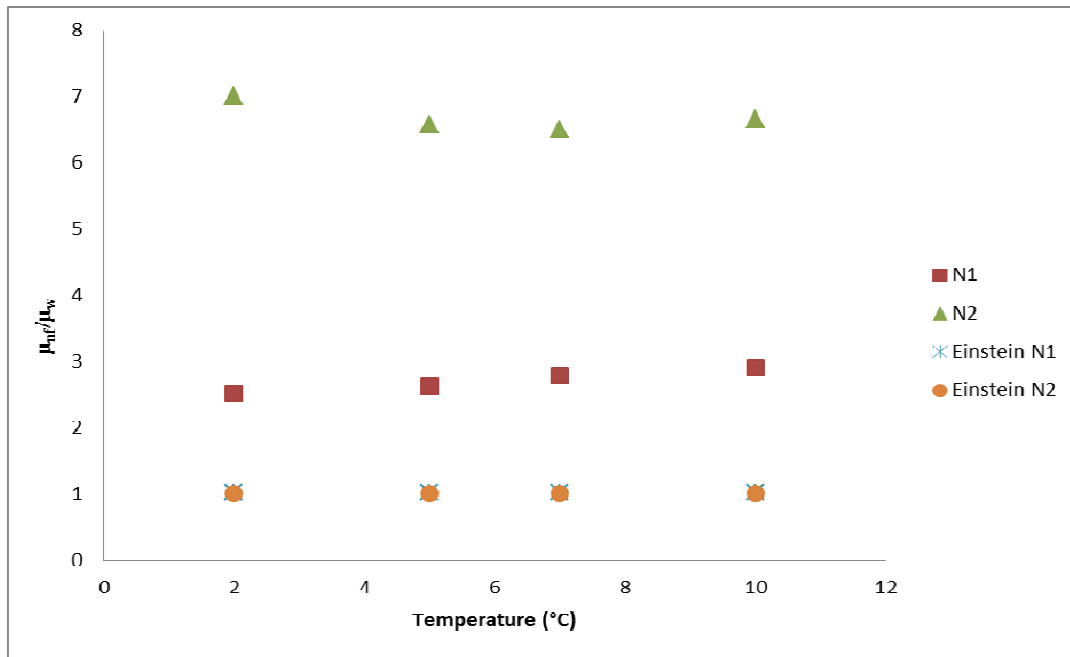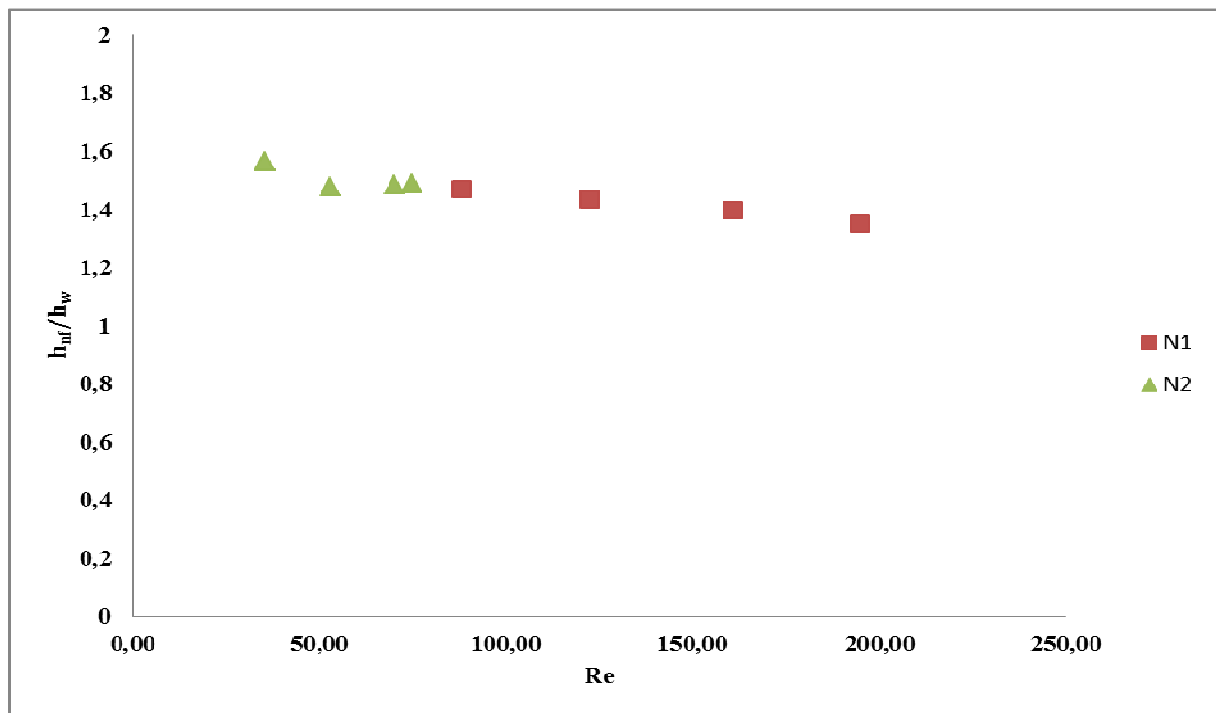*Figure 4 :*
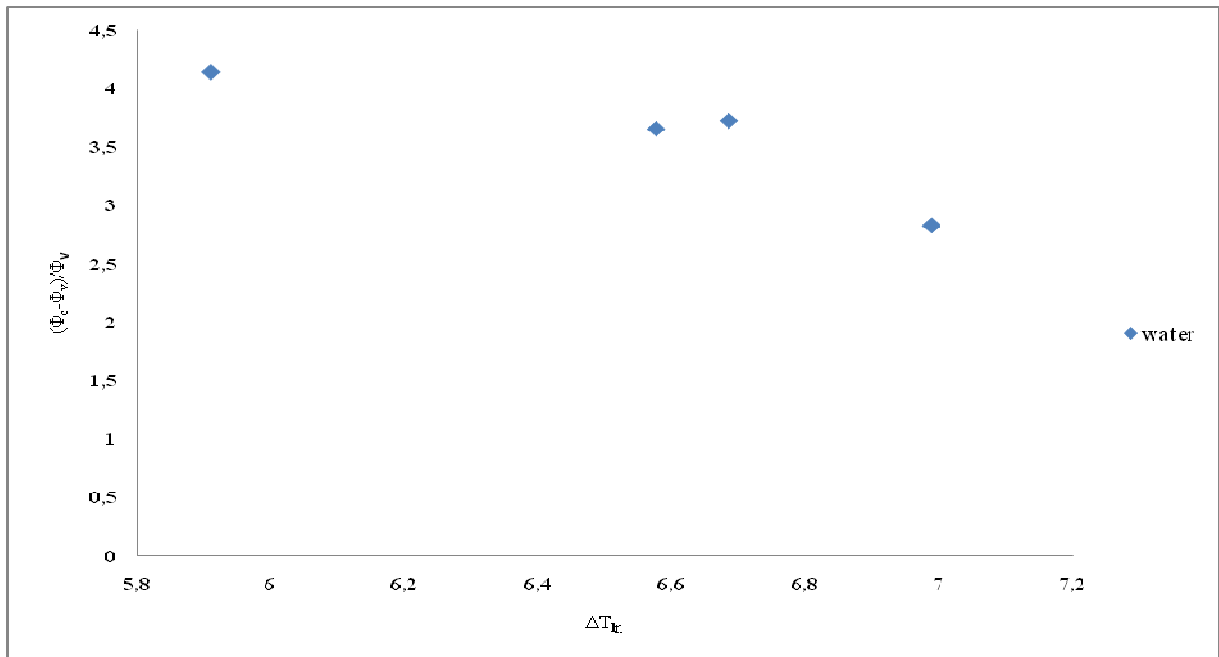
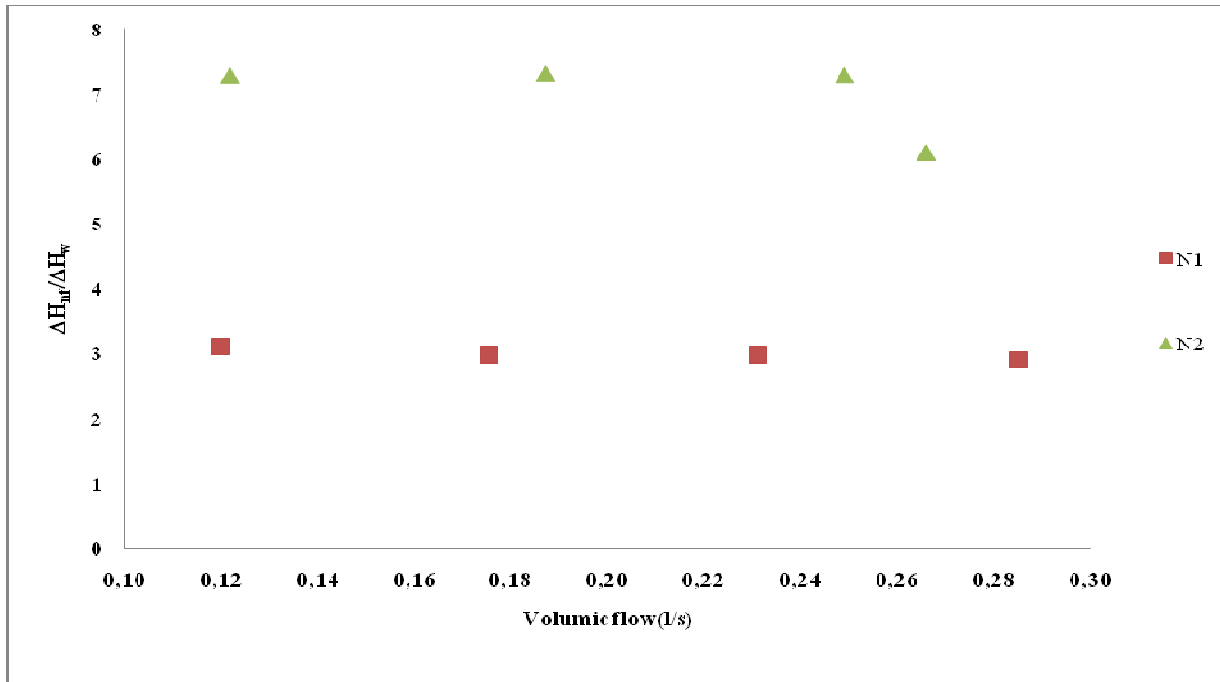*Figure 5 :*
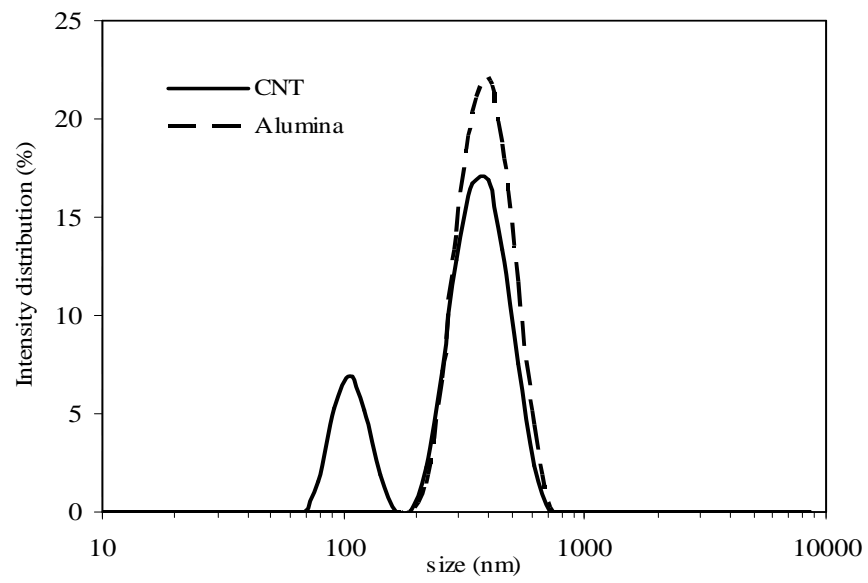
Figure 6 :

Figure 7:

Figure 8 :

Figure 9:

Figure 10:

Figure 11 :
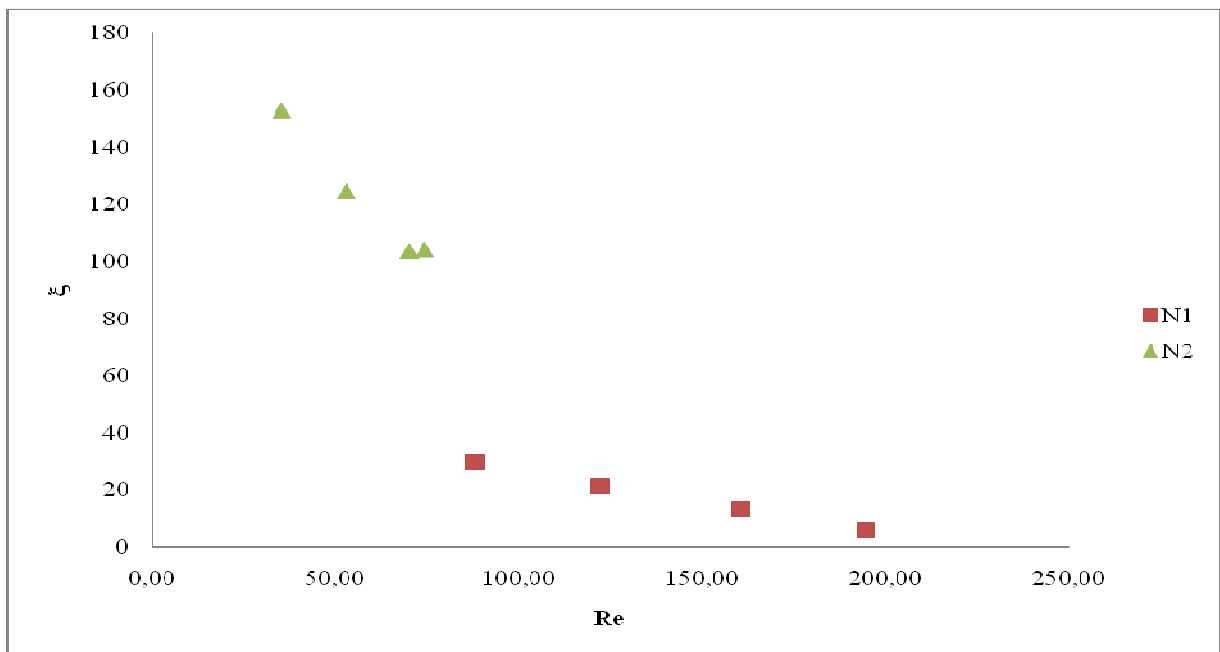
Figure 12 :

	Manufacturer name	Nanofluid	diameter (nm)	φ_v	Surfactant
N1	nanoteK A1121W	Aqueous alumina (γAl_2O_3)	37	1	1% wt* Unknown
N2	Aquacyl MSDS	Aqueous Carbon Nanotube CNT	9-10 2µm length	0.55	2% wt* SDBS

(*) : mass concentration

Table 1 :

Nanofluid	Flow regime	$(h_w - h_{nf})/h_w$
N1	Laminar Re=85 à 195	42%
N2	Laminar Re=35 à 75	50%

Table 2 :